

Local Surface Potential on Amorphous Silicon Thin Film Solar Cells by Kelvin Force Microscope

Takashi Itoh, Takanori Ito, Hiroshi Kuriyama and Shuichi Nonomura

Gifu Univ.

1-1 Yanagido, Gifu 501-1193, Japan

Phone: +81-58-293-2680 E-mail: itoh@gifu-u.ac.jp

Abstract

Local surface potential on hydrogenated amorphous silicon (a-Si:H) solar cells have been evaluated by Kelvin force microscope (KFM). Surface potential distribution was observed in surface potential image for pin a-Si:H solar cells. The difference between average of surface potential on n-type $\mu\text{-Si:H}$ and that on pin a-Si:H solar cell increased with increasing built-in potential. The difference between local surface potential on large convex grains was smaller than that in the region between the large convex grains.

1. Introduction

In silicon thin film solar cells, microcrystalline materials such as hydrogenated microcrystalline silicon ($\mu\text{-Si:H}$) are used as photo-absorption layer and doped layer materials. The $\mu\text{-Si:H}$ has hetero-structure composed of amorphous silicon (a-Si), crystalline Si grains, and grain boundaries. Typical Si thin film solar cells are prepared on glass substrates coated with textured transparent conductive oxide (TCO). Thus, the local properties in Si thin film solar cells would be different due to above effects. Therefore, we have investigated local properties of Si thin films and Si thin film solar cells by scanning probe microscope (SPM). Kelvin force microscope (KFM) is one of SPM techniques. The surface morphology and surface potential images can be obtained simultaneously. Previously, we reported that local surface potential is not uniform on $\mu\text{-Si:H}$ films [1]. We also reported the local surface potential distribution was observed on a-Si:H solar cells under light irradiation [2].

In this work, the local potential on a-Si:H solar cells was evaluated by KFM.

2. Experimental Methods

The samples evaluated in this work were a-Si:H solar cells which structure was Asahi U-type substrate / n-type $\mu\text{-Si:H}$ / i-type a-Si:H / p-type $\text{a-Si}_{1-x}\text{C}_x\text{:H}$. Here, Asahi U-type substrates were glass coated with textured SnO_2 .

KFM measurements were performed in air at room temperature (around 25 °C) using SPM-9600 (Shimadzu). Pt coated Si cantilevers (Olympus, OMCL-AC240TM-R3) were used as a probe. In the KFM measurement, the probe scanned on the free surface of the n-layer.

3. Results and Discussion

Figure 1 shows (a) surface morphology and (b) surface potential images for pin a-Si:H solar cell without light irradiation. In the surface morphology images, large convex grains were observed as shown in Fig. 1(a). The large convex grains correspond to the textured surface of Asahi U-type substrates. In the surface potential images for the pin a-Si:H solar cell, the local surface potential on the large grains was smaller than that in the concave region between the large grains as shown in Fig. 1(b).

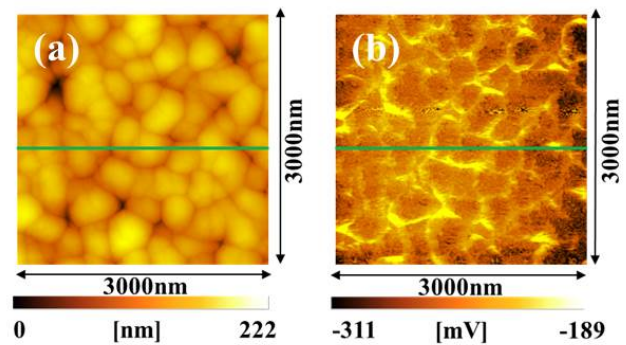


Fig. 1 (a) Surface morphology and (b) surface potential images for pin a-Si:H solar cells without light irradiation.

Figure 2 shows (a) surface morphology and surface potential images for n-type $\mu\text{-Si:H}$ films deposited on Asahi U-type substrates without light irradiation. The surface potential distribution obtained on the pin a-Si:H solar cells was similar to that obtained on n-type $\mu\text{-Si:H}$ films. The value of the surface potential on pin a-Si:H solar cells, however, was different from that on n-type $\mu\text{-Si:H}$ films. The difference between surface potential on n-type $\mu\text{-Si:H}$ and that on pin a-Si:H solar cell would correspond to built-in potential in a-Si:H solar cells. So, we measured surface potential images on n-type $\mu\text{-Si:H}$ films and pin a-Si:H solar cells deposited on Asahi U-type substrates by KFM. Then, the difference between average of surface potential on n-type $\mu\text{-Si:H}$ and that on pin a-Si:H solar cell was obtained. The difference between average of surface potential on n-type $\mu\text{-Si:H}$ and that on pin a-Si:H solar cell increased from 0.26V to 0.77V with increasing built-in potential from 0.61V to 1.30V. Based on this result, built-in potential was able to be evaluated from difference between

surface potential on n-type $\mu\text{-Si:H}$ films and that on pin a-Si:H solar cells by KFM. The difference between surface potential on n-type $\mu\text{-Si:H}$ films and that on pin a-Si:H solar cells by KFM, however, was smaller than the built-in potential. The KFM measurements were conducted in air. Therefore, this might be related to oxidization of free surface of the samples.

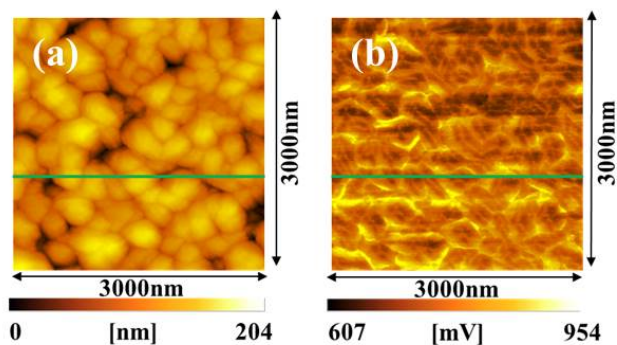


Fig. 2 (a) Surface morphology and (b) surface potential images for n-type $\mu\text{-Si:H}$ films without light irradiation.

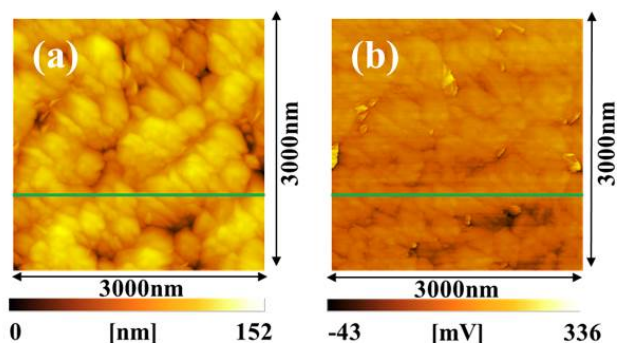


Fig. 3 (a) Surface morphology and (b) surface potential images for p-type $\text{a-Si}_{1-x}\text{C}_x\text{:H}$ films without light irradiation.

As written above, the surface potential distribution on pin a-Si:H solar cells was observed. Using above method, the local built-in potential was able to be evaluated in a-Si:H solar cells. Therefore, the difference between the surface potential on large convex grains for pin a-Si:H solar cells and that for n-type $\mu\text{-Si:H}$ films deposited on Asahi U-type substrates was obtained. The difference between the surface potential in the region between the large convex grains for pin a-Si:H solar cells and that for n-type $\mu\text{-Si:H}$ films deposited on Asahi U-type substrates was also obtained. The local built-in potential on large convex grains was smaller than that in the region between the large convex grains. This result would be explained by the difference between p-type $\text{a-Si}_{1-x}\text{C}_x\text{:H}$ and n-type $\mu\text{-Si:H}$ films deposited on Asahi U-type substrates. Figure 3 shows (a) sur-

face morphology and (b) surface potential images for p-type $\text{a-Si}_{1-x}\text{C}_x\text{:H}$ films deposited on Asahi U-type substrates without light irradiation. In Fig. 3, the local surface potential on the large convex grains was larger than that in the region between the large convex grains. This tendency was reverse one against that on n-type $\mu\text{-Si:H}$ films deposited on Asahi U-type substrates. The difference between surface potential on p-type $\text{a-Si}_{1-x}\text{C}_x\text{:H}$ and that on n-type $\mu\text{-Si:H}$ would be related to the built-in potential in a-Si:H solar cells. Therefore, the local built-in potential on the large convex grains was smaller than that in the region between the large convex grains.

Both of the local built-in potential in surface potential on large convex grains and that in the region between the large convex grains increased with increasing the built-in potential. The difference between the local built-in potential on the large convex grains and that in the region between the large convex grains in a-Si:H solar cells with large built-in potential was smaller than that with small built-in potential. These results suggest that the properties would be affected by the local properties in pin a-Si:H solar cells.

4. Summary

We demonstrated that built-in potential can be measured by KFM. In pin a-Si:H solar cells, the local built-in potential on the large convex grains was smaller than that in the region between the large convex grains. The difference between the local built-in potential on the large convex grains and that in the region between the large convex grains in a-Si:H solar cells with large built-in potential was smaller than that with small built-in potential. Based on these results, the macro properties would be affected by the local properties in pin a-Si:H solar cells.

Acknowledgements

This work was supported partially by SENTAN, JST.

References

- [1] T. Itoh, et al., *Renewable Energy 2010 Proc.* (2010) P-Pv-49.
- [2] T. Itoh, et al., *J. Phys. : Conf. Series* **379** (2012) 012003..